Possible clustering in space and time of aftershocks of the ML 5.7 Lake Muir earthquake, southwest Australia, 16 September 2018

Vic Dent[1], David Love[2] and Clive Collins[3]

1. University Associate, Curtin University, Perth, W.A.: Hon. Research Associate, Institute of Agriculture, University of Western Australia, Perth.; Email: vic_dent@yahoo.com

2. Seismological Association of Australia, Adelaide, South Australia; Email: david@earthquake.net.au
3. GPO Box 2972, Canberra ACT 2601; Email: collins@pcug.org.au

ABSTRACT

An ML 5.7 earthquake occurred NW of Rocky Gully, in southern WA on 16 Sep 2018 and formed a N-S trending surface rupture, visible intermittently over about 5 km. The event was followed by a ML 5.3 event about 7 weeks later. Geoscience Australia (GA) installed 5 field stations 4 days after the main event, and recorded about 900 mostly small aftershocks over the following 5 months. Events located before the installation of the field network, including the main event, have poor locations. GA has used the hypo-double difference method to relocate 470 aftershocks recorded by the Lake Muir network. Their results suggest a concentration in the north, presumably related to the main event, and also events with an apparent SW trend in the south, presumably related to the second (strike slip) event. GA's phase data are used here to relocate all 33 of the larger events (ML ≥ 2.3) from 20 Sep 2018 – 11 Feb 2019, and about 20 of the smaller events, using a different earth model. A suggested improved location for the ML 5.3 event is ~ 3 km southwest of the GA location, and closer to the scarp and other aftershocks. The relocations presented here show less scatter than the original data set. The progression in space of the events over time is discussed in this report. The improved epicentral data set seems to strengthen the case for Clark et al's. interpretation of a northeast trending strike slip fault for the ML 5.3, 8 November event, though support for s south-east dipping fault plane for the ML 5.7 event seems limited.

1 INTRODUCTION

The south-western area of Western Australia where the Lake Muir events occurred (Figure 1) is in the far south of a region known as the southwest seismic zone (SWSZ) (Doyle, 1971). The southern part of the seismic zone has been generally regarded as having lower seismicity than the northern part (eg. Burbidge et al., 2012, Figure 1). The boundary between the Yilgarn Craton (to the north), and the Albany-Fraser Orogen (to the south) bisects the region.

The first seismograph in the south of Western Australia (RKG) was installed near Rocky Gully in 1984, and seismicity of the region prior to this was very poorly monitored. The closest station to the Lake Muir area prior to 1980 was at Narrogin, some 200 km to the north. Earthquakes in the region, ML 2.5 and above, from 1980 – 2017 are shown on Figure 1. An ML 3.2 event occurred south of Lake Muir in 1980 (prior to the installation of RKG) and this epicentre has large uncertainties in location – perhaps +/- 40 km. A study of clustered seismicity in SW Western Australia from 1990 – 2015 (Dent, 2016) shows only one cluster in the region, north of Rocky Gully in 2013 (location T on Figure 1), although there was another just north of the region (southwest of Kojonup) in 1999.

On 16 Sept 2018, a magnitude (ML) 5.7 event occurred about 30 km north of Rocky Gully. It was the largest West Australian earthquake since the magnitude (ML) 5.6 event south of Norseman in July 2016 (Dent & Love, 2018), and the first magnitude 5 event in south-west WA since the Burakin earthquakes of March 2002 (Leonard, 2003). As described by Clark et al. (2019), a temporary network of 5 recorders installed by GA four days after the

main event enabled the location of ~800 aftershocks in the following 5 months. This included a ML 5.3 event on 8 Nov 2018. This deployment has allowed a relatively rare opportunity to investigate the aftershocks of a large Australian earthquake in moderate detail. Previous well-studied events, which have revealed fault-plane orientations, include the ML 4.1 Eugowra NSW event of 1994 (Gibson et al., 1994, 8 recorders), and the ML 6.8 Tennant Creek NT event of 1988 (Bowman, 1992, 10-20 recorders).

Most of the Lake Muir aftershocks recorded by GA were quite small, with over 80% beeing less than ML 1.5. Activity dropped off significantly after mid-November 2018. A time vs. magnitude plot of the earthquake sequence until February 2019 is shown in Figure 2. No epicentres are listed in the GA catalogue since February 2019, however small and unlocatable events are still being felt at de Campos farm (Figure 1, Rob de Campos, pers. comm., Sept 2019).

Figure 1. Seismicity in the Lake Muir area, 1980 - 2017 (geology after Clark et al., 2019). Insert shows hazard levels in SWSZ, from Burbidge et al., (2012).

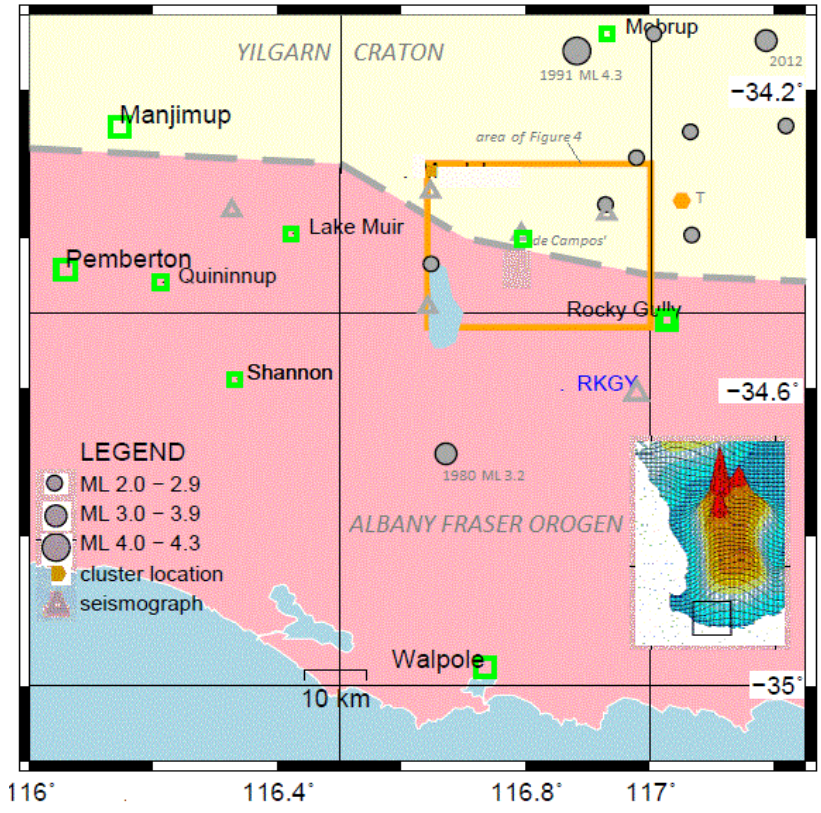

Clark et al., (2019) present relocations for 470 events. These relocations, for the period 20 Sep to 23 Nov 2018, used data from the Lake Muir (LM) field stations, and were calculated by the hypo double difference (HypoDD) method (Waldhauser and Ellsworth, 2000) This technique is intended to produce a data set with more reliable locations, by using relative differences in phase arrivals for neighbouring events. It does not use calculated travel times for individual events to produce a location.

In this report the seismicity near Lake Muir between Aug 2018 and Feb 2019 is analysed in four time periods (periods 1 to 4, Figure 2), which were chosen to capture significant developments in the seismically active period and its monitoring. The objective is to see if there are meaningful trends in the aftershock distribution. Clark et al., (2019) states "in statistical seismology the uncertainties attached to the calculated locations of small to moderate sized events forming part of a sequence typically precludes analysis of the detailed temporal, spatial and/or structural relationships between failure surfaces, even with dense instrument networks." However the Eugowra sequence shows that with sufficient recorders, suitably placed, one can estimate the extent of the rupture, its dip and aftershock migration over time (Gibson et al., 1994).

Most of the events discussed in this report have been relocated using EQLOCL, an earthquake location program developed by the Seismology Research Centre (SRC), Melbourne, and used by GA for its routine earthquake locations between ~1991 and 2015. Earthquake solutions are variously described as "good" or "poor", and this is relative to location accuracies normally achieved by the Australian National Seismograph Network (ANSN), operated by Geoscience Australia. Most of the solutions presented, which include data from several stations of the local Lake Muir network, are "good" in that the RMS of residuals is low (< 0.05 secs), and a location uncertainty of < 0.5 km can be expected.

In cases where there is only one local station used, or none, locations may be poor, because there are not enough data to adequately resolve the location of the earthquake. Location uncertainties rise to ~ +/- 5 km, and perhaps +/- 10 km if there is no local data at all. Local network data is not universally available over the time period studied, because of factors like poor weather, or shading on the solar panels used to power the recorders. When the largest azimuthal gap between recorders is >180° accuracy decreases significantly. For accurate depths to reveal rupture planes, the epicentral distance to the nearest station needs to be less than the event depth.

Figure 2. Time V Magnitude plot for the Lake Muir sequence. "Other" data from a review of RKGYdata

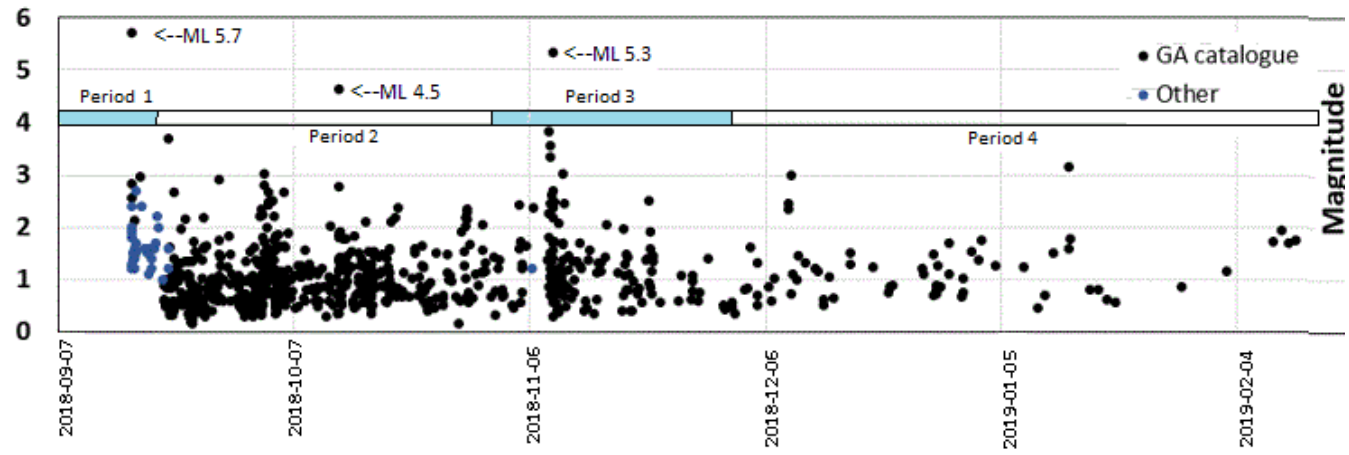

Events selected for relocation using the HypoDD program needed to meet strict criteria (> 8 phases). It is not clear if the largest aftershocks, ie. the earthquakes treated in this report, were relocated by this method. The map produced by Clark et al. (2019) indicated a concentration of aftershocks near LM01, and a southwest trend noticed in events further south was interpreted as following the strike-slip fault, inferred for the ML 5.3 event from focal mechanism studies.

Figure 3. P wave velocity Vs depth models

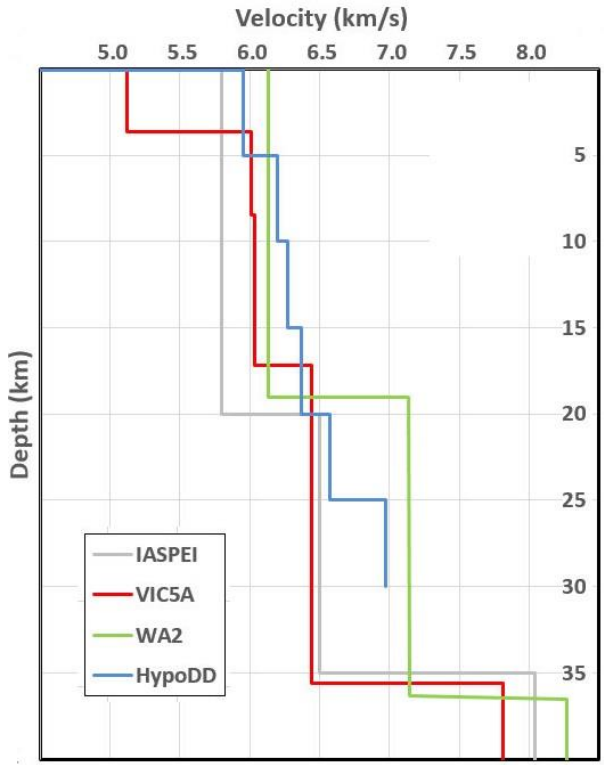

A new earth model was devised for the HypoDD relocations (Clark et al., 2019), which was based on research of Dentith et al. (2000) and Salmon et al. (2013). This model (Figure 3) has relatively high values for the P wave velocity (varying from 6.20 km/sec at 5 km depth to 6.37 at 15 km). The WA2 (Dent, 1989) and VIC5A (V. Wesson & G. Gibson, pers. comm., 1986) models, which are also used later in this report, are also shown in Figure 3. The VIC5A model was developed by the SRC for central Victoria, and has a relatively low velocity layer near the surface. This shallow near-surface layer suits the suggestion by Somerville & Ni (2010) that a shallow low velocity layer is required to explain the observed Raleigh waves in southwest Australia. The WA2 model uses a P wave velocity of 6.13 km/sec for the depth range 0 to 19 km. However, the VIC5A model has even lower velocities, but seems to produce the best

results – ie. lowest RMS of residuals, and depths which do no tend to rise above the surface.

The locations of the largest 24 events (ML 2.5 and above), and selected smaller events are reviewed in this report.

2 ALTERNATIVE LOCATIONS OF THE THREE LARGEST EVENTS (ML's 5.7, 5.3 and 4.6)

This analysis begins by reviewing published locations for the three largest events, ie. 16 Sept (ML 5.7), 12 Oct (ML 4.6) and 8 Nov (ML 5.3) 2018. The best locations are probably those by GA, but there were also locations by the USGS (Boulder, Colorado), the European-Mediterranean Seismological Centre (EMSC, Strasbourg) and the Seismology Research Centre, Melbourne. These other agencies used only Australian National Seismograph Network (ANSN) stations – ie. they did not use Lake Muir field station data. The various solutions for the events are shown in Table 1 and Figure 4, and will now be examined in more detail.

A rough guide to the quality of the locations is the residual at Rocky Gully (RKGY, the closest ANSN station, about 30 km southeast) – ideally the residual at RKGY (column 9 in Table 1) should be less than about 0.2 secs, and larger values indicate suspect solutions. The other guide is the RMS of residuals for the location as a whole (column 8 in Table 1). This should be under ~ 0.5 secs, but is much larger for most of the solutions because inappropriate crustal models, and/or possibly poor data from remote stations, have contributed to the uncertainties of the locations.

Figure 4. Locations by different agencies for the 3 largest events

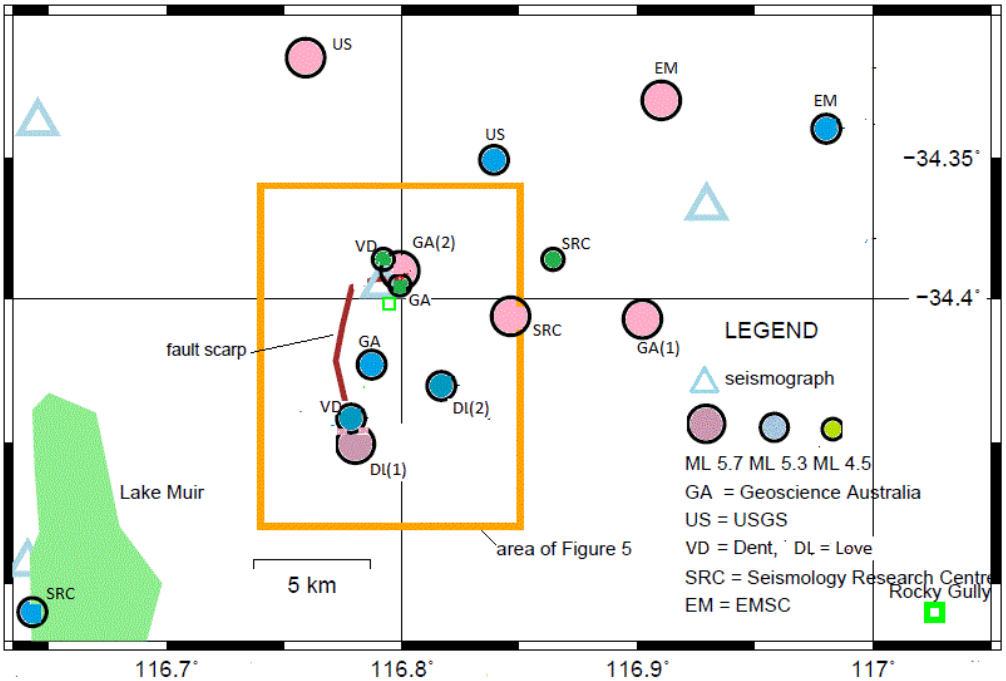

ML 5.7 event, 16 Sep 2018, 0456 UTC (red solutions, Figure 4)

The solutions for this event vary widely (dispersed over ~ 20 km) but most can be considered poor because there were no close stations other than RKGY, and RKGY generally has a large residual (> ~ 0.5 secs). The Lake Muir network was not yet installed. There are two solutions for this event in Table 1 by GA. GA (1) is the solution found in the database (https://earthquakes.ga.gov.au/), and uses only the ANSN stations. GA (2) is presented by Clark et al., (2019) and includes data from the nearby infrasound station at Shannon. Clark et al. (2019) indicate an error ellipse of diameter ~ 15 km, but the solution seems to be good because of its proximity to following events and the surface rupture.

A single station solution for the ML 5.7 event (DL1 on Figure 4) was calculated using the P arrival of the RKGY waveform. Using the rotation function in "Waves" (src.com.au) and minimising the early P arrival (10 samples) on the East axis an angle of 314+/- 3^{o} was estimated. An effective S-P time (where the S wave is related to the P) of 2.99 sec. was used.

ML 5.3 event, 8 Nov 2018, 2107 UTC (blue solutions, Figure 4)

As with the ML 5.7 event 7 weeks earlier, the published solutions of the main agencies (GA, USGS, EMSC and SRC) for this event are widely scattered. The GA solution uses field station data (but not LM01 or LM02) and is the best of the group. The relocation presented later in this report (labelled VD), is about 2 km SW of the GA location, and on the other (south) side of the mapped rupture. The single station solution (DL2) is also shown on Figure 4.

ML 4.6 event, 12 Oct 2018, 1631 UTC (green solutions, Figure 4)

This event occurred about half way through the sequence between the two large (ML 5+) events. The GA solution for this event (which uses LM field data) is about 1 km east of LM01. The depth given is 6 km, and the RMS of residuals is 0.45 sec. A relocation for this event (labelled VD) presented later is this report, and using LM network data only, is very close to the GA location, about 1 km north of LM01.

Table 1. Solutions from different agencies for the 3 largest Lake Muir events of 2018

Date	Agency	Lat. deg. Sth.	Long. deg E.	Depth (km)	Stns /phases	Gap (deg)	RMS (sec)	RKGY resid.	Model	Remarks
16 Sep	GA (1)	-34.407	116.902	2.0	93/96	39	1.40		IASPEI	GA catalogue
16 Sep	GA (2)	-34.390	116.799	0.0						Uses infra-sound
16 Sep	USGS	-34.315	116.759	10.0	?/99	42	1.4	--		Closest stn 160 km
16 Sep	EMSC	-34.330	116.910	2.0	186/194	33	1.45	-1.2		
16 Sep	SRC	-34.404	116.851	5.1	20/24	148	0.47	-0.55	WA2	
12 Oct	GA	-34.395	116.799	6.0	12/18	88	0.45		IASPEI	Uses LM net
12 Oct	SRC	-34.386	116.842	5.3	21/26	143	0.37	-0.18	WA2	
12 Oct	VD	-34.386	116.792	1.4	5/6	149	0.055	-0.41	VIC5A	Uses LM net
08 Nov	USGS	-34.351	116.839	10.0	?/61	61	0.97	--		Closest stn 162 km
08 Nov	EMSC	-34.340	116.980	10.0	101/107	48	1.60	-1.9		
08 Nov	SRC	-34.510	116.643	10.0	17/21	262	1.20	0.74	WA2	
08 Nov	VD	-34.438	116.777	0.5	6/9	142	0.12	0.05	VIC5A	Uses LM net

3 DISTRIBUTION OF AFTERSHOCKS OVER TIME

The seismicity is divided into 4 time periods. Period 1 includes the foreshock, mainshock, and aftershocks recorded before the Lake Muir network was in operation (ie. up to 19 Sep). Period 2 is between 20 Sep and 31 Oct, and Period 3 is between 1 and 30 Nov, a period which includes the second big event (ML 5.3 on 8 Nov). Period 4 is the tail of the activity from 1 Dec 2018 to 11 Feb 2019, when the LM network was removed. All events of ML 2.3 and above have been relocated using EQLOCL, as well as ~20 of the smaller ones.

3.1 Period 1 - 1 Aug to 19 Sep 2018

The seven events of this period, including the ML 5.7 event of 16 Sep are shown in Table 2 and Figure 5. They are poorly located, as they occurred before the installation of the Lake Muir network, i.e. the locations rely solely on the widely spaced ANSN network. The events are scattered, and mostly remote from the activity of the following weeks, but if they were well-located, they would probably be in the vicinity of the scarp, and probably close to LM01. The first event (foreshock) of 30 Aug (ML 2.3) was recorded by only 3 stations and is particularly poorly located. Although there are only 4 events in the catalogue for the period 16 to 20 Sep 2018, it can be expected that a large number of small events would have been recorded had the temporary network been in place at the time (see Figure 2**,** "other events").

Fig 5. GA locations of events in Period 1 (01 Aug – 19 Sep 2018)

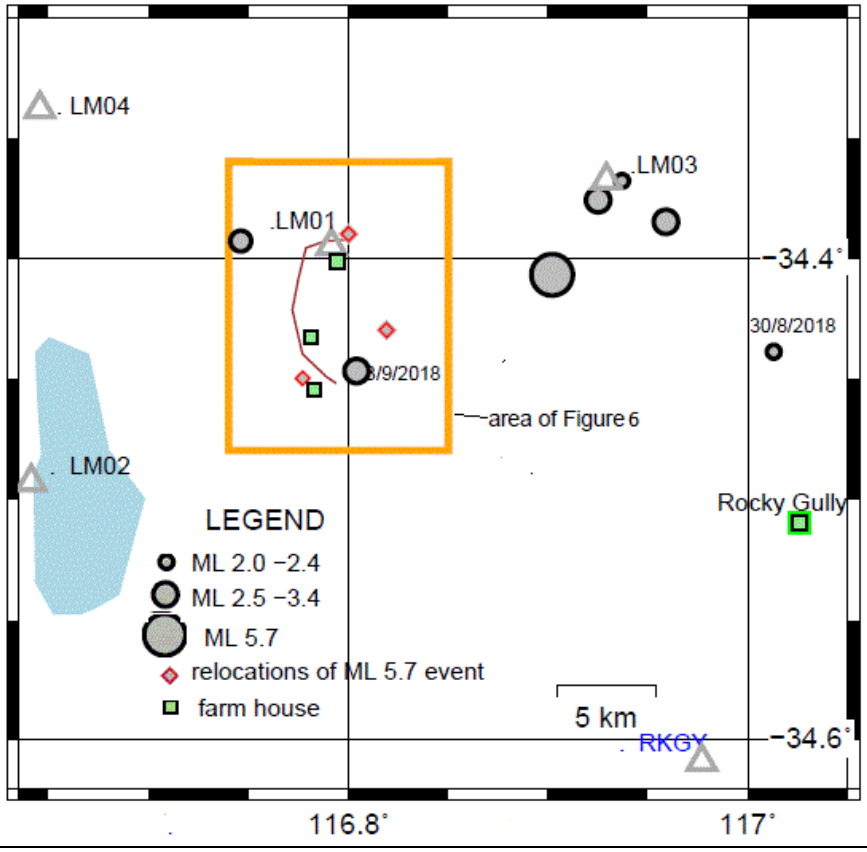

Table 2. GA locations in Period 1 (01 Aug – 19 Sep 2018) for all magnitudes

Date/Time (UTC)	GA		Mag (ML)	Depth (km)	Stations /phases	RMS (sec)	Comment
	Lat	Lon					
30 Aug 12:38	-34.439	117.013	2.3	10	3/5	0.55	Foreshock
13 Sep 18:15	-34.447	116.804	3.4	10	9/13	0.7	Foreshock
16 Sep 04:56	-34.407	116.902	5.7	1.7	93/96	1.4	Largest event
16 Sep 05:23	-34.385	116.959	2.8	2.9	5/9	0.9	
16 Sep 07:07	-34.376	116.925	2.6	1.0	3/6	0.26	
16 Sep 13:11	-34.368	116.937	2.1	1.0	3/6	0.24	
17 Sep 07:09	-34.393	116.746	3.0	1.0	6/9	1.1	

3.2 Period 2 - 20 Sep to 31 Oct 2018

This section reviews the initial 6 weeks of data acquired by the temporary network. GA has located ~560 events in this period, of which 81 were ML 1.5 or larger (Figures 6). The northern region is shown in more detail in Figure 7. There were 11 events of ML ≥ 2.5, which have been relocated, and these are listed in Table 3. The two largest events were ML 3.7 (on 20 Sep, the day the Lake Muir network, and this period, started) and ML 4.6 on 12 October. Table 3 suggests a concentration of events on 20-21 September (perhaps a tailing-off of activity from the 16 September ML 5.7 event) and another concentration on 2-4 October. This latter group is also visible on Figure 2, and the largest event was ML 3.0 on 03 October. They are mainly north of de Campos' farm, and the relocations suggest a possible northeast lineation.

Table 3. Locations/relocations of events in Period 2, 20 Sep – 31 Oct 2018. All events ML > 2.4, plus selected extra events of lower magnitude)

Date/Time (UTC)	GA		Mag (ML)	Depth (km)	RMS (sec)	Relocation		Depth (km)	RMS (sec)	
	Lat	Lon				Lat	Lon			
September										
20 2220	-34.416	116.826	3.7	8	1.20	-34.412	116.785	0.7	.11	2nd largest
21 0104	-34.411	116.780	1.6	2.7	0.07	-34.406	116.779	2.2	.05	
21 0954	-34.431	116.794	1.1	2.5	0.05	-34.422	116.790	2.8	.025	
21 1437	-34.415	116.777	2.7	2.4	0.66	-34.407	116.777	2.2	.04	
22 1836	-34.452	116.775	0.5	1.5	0.18	-34.400	116.784	2.2	.005	Big move
27 1002	-34.389	116.793	2.9	3.0	0.42	-34.386	116.796	1.6	.03	
30 1208	-34.477	116.791	0.6	0	0.22	-34.417	116.796	2.7	.03	Big move
October										
02 0848	-34.457	116.781	1.3	2.4	0.07	-34.459	116.777	0.8		
02 2024	-34.381	116.810	2.3	1.8	0.70	-34.388	116.802	1.9	.05	
03 0240	-34.406	116.795	1.5	2.5	0.12	-34.396	116.799	2.7	.04	
03 0315	-34.401	116.808	2.8	3.9	0.6	-34.385	116.801	1.8	.03	
03 0341	-34.387	116.806	3.0	4.1	0.35	-34.384	116.800	1.9	.04	
03 15:26	-34.391	116.784	2.7	3.3	0.33	-34.395	116.788	1.6	.035	
03 1551	-34.39	116.809	2.4	1.3	0.56	-34.389	116.803	2.1	.05	
03 1726	-34.386	116.800	2.5	2.8	0.16	-34.388	116.801	.21	.045	
04 0741	-34.395	116.807	2.5	1.5	0.45	-34.396	116.801	2.7	.03	
04 1638	-34.412	116.792	1.7	2.2	0.18	-34.404	116.792	1.9	.055	
05 15:14	-34.378	116.796	2.7	3.2	0.34	-34.387	116.799	2.4	.04	
12 16:31	-34.395	116.799	4.6	5.8	0.45	-34.386	116.792	1.4	.07	largest
12 16:40	-34.381	116.797	2.8	1.6	0.58	-34.392	116.795	1.9	.08	
19 0755	-34.463	116.782	2.1	1.6	0.78	-34.452	116.786	2.1	.02	
19 1932	-34.456	116.776	2.2	2.6	0.45	-34.456	116.788	2.1	.05	
29 0104	-34.449	116.783	2.3	2.8	0.18	-34.451	116.784	2.1	.05	

The ML 3.7 event on 20 September seems poorly located, and the relocation moves it about 4 km westward, closer to other events, and the focal depth changes from 8 km to ~ 1 km. The relocation of the ML 4.5 event on 12 October moves it only slightly, but brings it in to the north-east trend suggested above. Another possible grouping

of events occurs at the end of October, and these events seem to fall at the far south of the mapped scarp.

While there are relatively few events south of 34.42ºS in October 2018, the GA plot shows they did occur, but
were mostly low magnitude (ML < 1.5). Four of the smaller events were relocated (Table 3), and three of the relocations moved the events significantly further north, closer to the other events (Figure 6).

Figure 6. GA Locations for all events in Period 2 (20 Sep – 31 Oct 2018), ML≥ 1.5

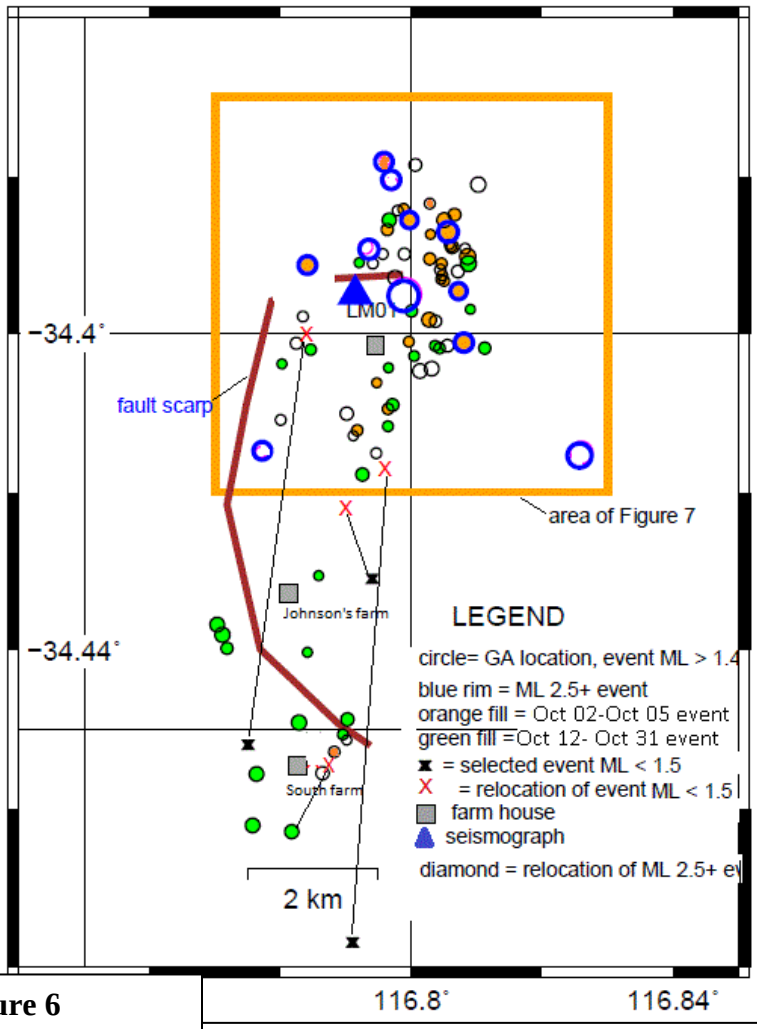

Figure 7. Enlarged boxed region of Figure 6

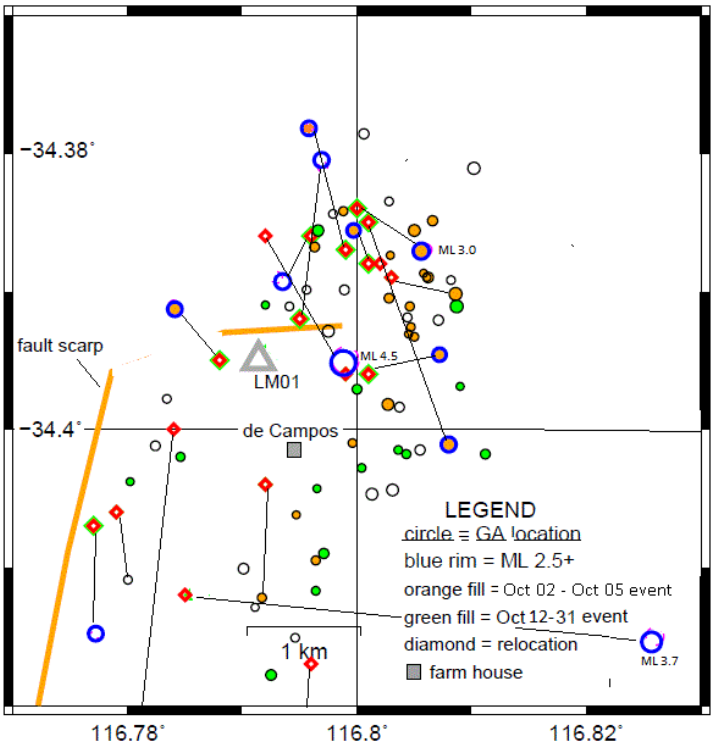

3.3 Period 3 - 1 to 30 November, 2018

The GA locations of events ML 1.5 and above, for Period 3 (1 Nov - 30 Nov) and Period 4 (1 Dec 2018 - 14 Feb 2019) are plotted on Figure 8**.** The two largest events (ML 3.8 and ML 5.3) were both on 8 November 2018 and there was a big spike of activity surrounding the ML 5.3 event. Period 3 was defined to begin on 1 November in order to allow for possible foreshocks of the ML 5.3 event. Figure 8 shows how the activity north of LM01, the dominant region of the previous period, has decreased, as is now represented by only three events.

Seismic activity was relatively low from mid-October to 7 November, the two notable events being ML 2.4 events on Nov 4 and Nov 6 (Figure 9). The ML 3.8 event at 1059 on 8 November, about 9 hours prior to the ML 5.3 event, heralded an increase in activity. The 30 events which were located by GA on 8 November (ML 0.3 – ML 5.3) are plotted on Figures 8 and 9 and listed in Table 4. Thirteen of these events have been relocated, including the two largest events. These relocations are shown in Fig. 9, and the two largest events have moved significantly (~ 3 km) to the southwest. The relocations in general seem to move the events towards the mapped fault scarp.

The amended distribution of events lies predominantly on the southwest side of the Sep.16 scarp. The relocations suggest they are all on the south side of the northeast trending strike slip fault (Figure 9) suggested by Clarke et al. (2019**)**, approximately though Johnson's farm, supporting that interpretation. Perhaps the true location of the fault is about 1 km south of that suggested by Clark et al. An ML 2.5 event on 21 November, north of LM01 (Figure 8), was accompanied by at least six other close events on that day and would seem to be a renewal of

Figure 8. GA locations of events ML ≥ 1.5 in periods 3 and 4, (01 Nov 2018 – 11 Feb 2019)

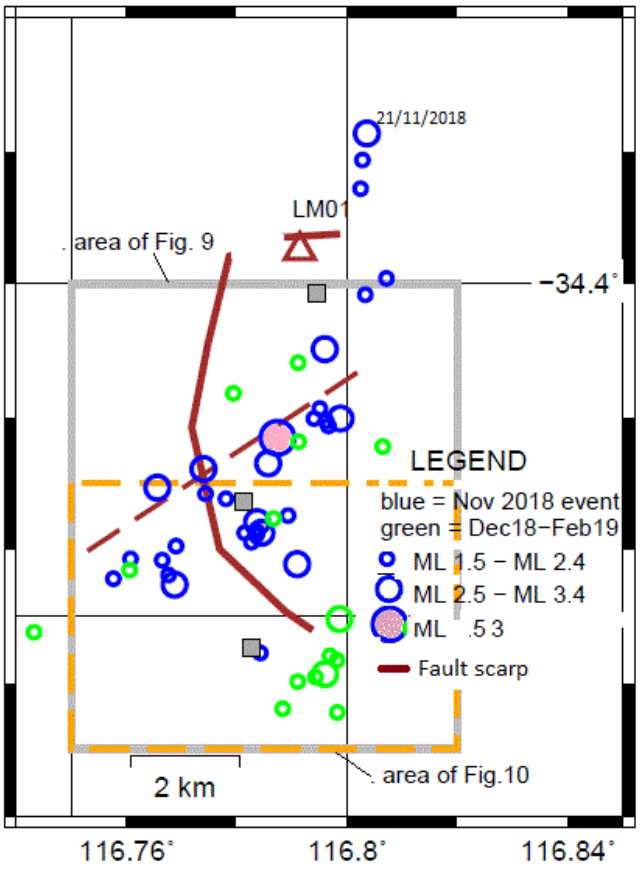

Figure 9. Events on 8 Nov 2018 (all magnitudes), and events between 9 Nov - 30 Nov 2018, ML ≥ 2.0.

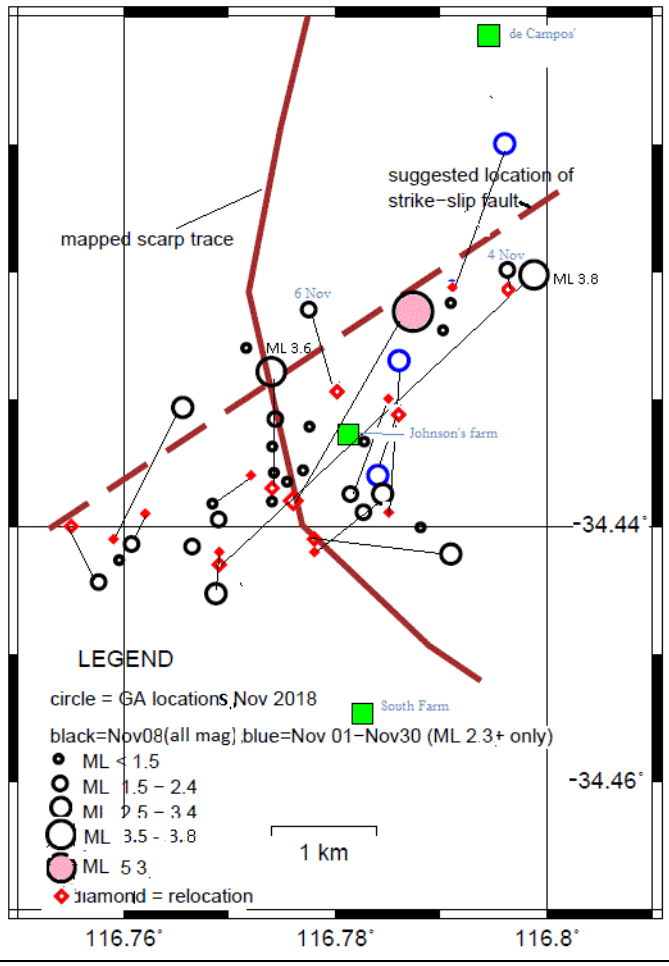

activity at the location of the early October 2018 activity at that location.

Table 4. Locations and relocations of Lake Muir region events in November 2018

Date (UTC)	Time (UTC)	Mag ML	GA		Depth (km)	RMS (sec)	Stations /phases	Relocation		Dept (km)	Remark*
			Lat	Lon				Lat	Lon		
Events on 8 November (all magnitudes)											
8-Nov	07:54:37	1.4	-34.422	116.791	2.9	0.017	5/6				
8-Nov	10:59:09	3.8	-34.420	116.799	3.0	1.17	24/29	-34.443	116.769	1.0	
8-Nov	11:01:24	2.3	-34.439	116.769	2.4	0.056	5/8	-34.436	116.772	2.3	
8-Nov	11:06:13	0.9	-34.438	116.768	2.6	0.06	5/10				
8-Nov	12:18:13	1.8	-34.432	116.774	2.7	0.3	6/11				
8-Nov	12:47:35	1.5	-34.442	116.766	1.5	0.17	6/11				
8-Nov	13:49:20	1.0	-34.420	116.796	2.7	0.15	5/10				
8-Nov	15:07:58	3.3	-34.442	116.791	4.0	0.61	11/12	-34.441	116.778	2.1	
8-Nov	15:09:34	3.6	-34.428	116.774	3.0	0.35	8/15	-34.437	116.774	1.5	
8-Nov	15:16:52	2.5	-34.437	116.784	3.0	0.79	8/10	-34.442	116.778	1.7	
8-Nov	15:30:35	0.7	-34.438	116.774	2.8	0.09	5/10				
8-Nov	15:45:02	1.0	-34.436	116.777	2.7	0.04	4/8				LM01 U/S
8-Nov	16:30:44	1.2	-34.434	116.774	2.5	0.04	4/8				LM01 U/S
8-Nov	16:40:07	1.1	-34.433	116.781	2.8	0.14	4/8				LM01 U/S
8-Nov	16:51:57	2.6	-34.445	116.769	1.8	0.31	7/12	-34.442	116.769	2.4	LM01 U/S
8-Nov	17:05:20	1.0	-34.433	116.783	3.1	0.16	4/8				LM01 U/S
8-Nov	18:50:45	0.9	-34.432	116.777	2.8	0.12	4/8				LM01 U/S
8-Nov	19:06:00	1.4	-34.436	116.775	2.5	0.03	4/8				LM01 U/S
8-Nov	21:07:00	5.3	-34.423	116.787	3.0	0.82	10/19	-34.438	116.777	0.5	LM01 U/S
8-Nov	21:14:42	2.7	-34.431	116.765	2.7	0.34	5/10	-34.441	116.759	2.1	LM01 U/S
8-Nov	21:23:24	1.7	-34.444	116.758	2.6	0.1	5/10	-34.440	116.755	3.6	
8-Nov	21:33:02	2.2	-34.441	116.761	2.6	0.05	5/9	-34.439	116.762	2.8	
8-Nov	21:43:27	2.4	-34.437	116.781	2.4	0.06	5/10	-34.430	116.785	1.9	
8-Nov	21:54:53	1.6	-34.439	116.783	2.4	0.05	5/9				
8-Nov	22:07:09	0.3	-34.376	116.772	4.0	0.006	3/6				3 stns only
8-Nov	22:34:30	0.6	-34.425	116.790	2.9	0.05	4/8				
8-Nov	22:35:49	0.6	-34.440	116.788	2.8	0.04	3/6				3 stns only
8-Nov	22:36:58	0.9	-34.443	116.759	2.4	0.04	4/8				
8-Nov	23:15:28	1.4	-34.426	116.772	2.7	0.03	5/10				
8-Nov	23:45:21	1.0	-34.436	116.774	2.8	0.06	5/10				
Other events in November 2018 (ML ≥2.3)											
4-Nov	16-21-30	2.4	-34.421	116.797	0.4	0.82	7/14	-34.422	116.797	1.7	
4-Nov	23-53-34	0.8	-34.473	116.793	0	0.24	3/6	-34.415	116.797	2.4	(low magn.)
6-Nov	11-00-10	2.4	-34.423	116.778	2.7	0.13	7/13	-34.430	116.780	2.7	
9-Nov	01-57-21	2.5	-34.410	116.796	1.2	0.68	8/14	-34.421	116.791	3.8	
10-Nov	04-51-12	3.0	-34.427	116.786	3.0	0.33	12/19	-34.439	116.785	2.1	
10-Nov	10-28-49	2.5	-34.436	116.784	1.7	0.44	9/15	-34.432	116.786	4.0	
21-Nov	02:22:14	2.5	-34.377	116.804	2.6	0.25	7/13	-34.385	116.803	2.8	N of LM01

*LM02 was U/S Nov06 – Nov10 2018

3.4 Period 4 1 Dec 2018 – 11 Feb 2019 (end-of-survey)

The seismicity declined significantly after 22 Nov 2018 (see time-magnitude plot, Figure 2), and the 15 GA locations (ML 1.5+) from 1 Dec 2018 to 11 Feb 2019 are shown in Figures 8 and 10 and listed in Table 5. Figure 10 shows most of the activity was at the southern terminus of the mapped scarp. There seem to be two principal periods of activity accompanying two magnitude 3+ events. The first (ML 3.0) on 9 December 2018 is poorly located as there were few phase arrivals. The second (ML 3.2) on 13 January 2019 was well located. It is possible, considering the location uncertainties, that the two events and their apparent aftershocks were co-located.

Scattered small events at other times in Period 4 seem to roughly correlate with the area of the strike slip fault.

Figure 10. GA locations, and relocations, in Period 4, (1 Dec 2018 to 11 Feb 2019), ML > 1.4

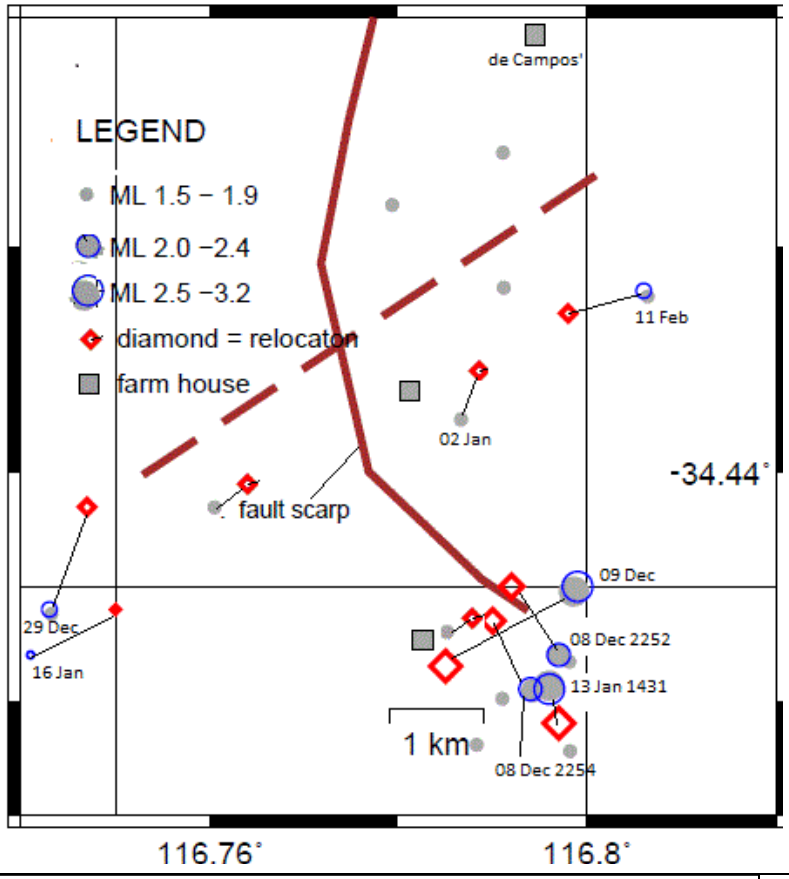

Table 5. Locations and relocations in Period 4, 1 Dec 2018 – 11 Feb 2019

Date (UTC)	Time (UTC)	GA solution		Mag (ML)	Depth (km)	RMS (sec)	Relocation		Depth (km)	RMS (sec)	
		Lat	Lon				Lat	Lon			
08-Dec	2252	-34.456	116.797	2.3	0.0	0.68	-34.45	116.792	4.2	0.059	
08-Dec	2254	-34.459	116.794	2.4	0.3	0.78	-34.453	116.790	2.3	0.013	
09-Dec	0613	-34.450	116.799	3.0	2.5	0.51	-34.457	116.785	2N	0.139	Poor data
16-Dec	2109	-34.443	116.760	1.5	2.7	0.07	-34.441	116.765	3.9	0.054	
27-Dec	1007	-34.454	116.787	1.5	2.4	0.01	-34.453	116.788	2.3	0.030	
29-Dec	0829	-34.452	116.743	1.7	2.2	0.06	-34.443	116.747	4.1	0.046	
02-Jan	1259	-34.435	116.787	1.8	1.8	0.14	-34.431	116.789	2.2		
13-Jan	1431	-34.459	116.796	3.2	3.9	0.42	-34.462	116.797	1.8	0.082	
13-Jan	1437	-34.457	116.798	1.6	3.1	0.07					
13-Jan	1906	-34.464	116.788	1.8	1.8	0.10					
16-Jan	0836	-34.456	116.741	0.8	2.5	0.08	-34.452	116.75	4.1	0.023	Low magn.
11-Feb	1555	-34.424	116.806	1.8	3.3	0.23	-34.426	116.798	2.2	0.038	

4 FOCAL MECHANISMS

First motion focal mechanisms were attempted for the two M5+ events (Figure 11). These included waveforms from many stations in Australia, particularly the GA and Seismographs in Schools network. Also, waveforms from some overseas stations available through IRIS were used. First motions reported to the International Seismological Centre (2019) On-line Bulletin were also used. The velocity model was VIC5A, reverting to IASPEI below 36km depth.

Most waveforms did not have clear arrivals. This is partly expected, since the hypocentres are relatively shallow, with near surface layering causing emergent arrivals.

The 16 Sep event is only moderately well constrained, with a significant number of first motions not fitting well. The preferred nodal planes are similar to the USGS nodal planes of their moment tensor focal mechanisms.

The 8 Nov event is poorly constrained, with many solutions possible. One possible solution, consistent with first motion being on the NE-SW plane suggested by Clark et al. (2019) is shown. In this case the nodal planes of the USGS moment tensor solution do not match well.

Figure 11. First motion focal mechanisms for the two M5+ events, lower hemisphere, showing nodal planes from USGS moment tensor solutions in blue, and preferred first motion nodal planes in dashed lines.

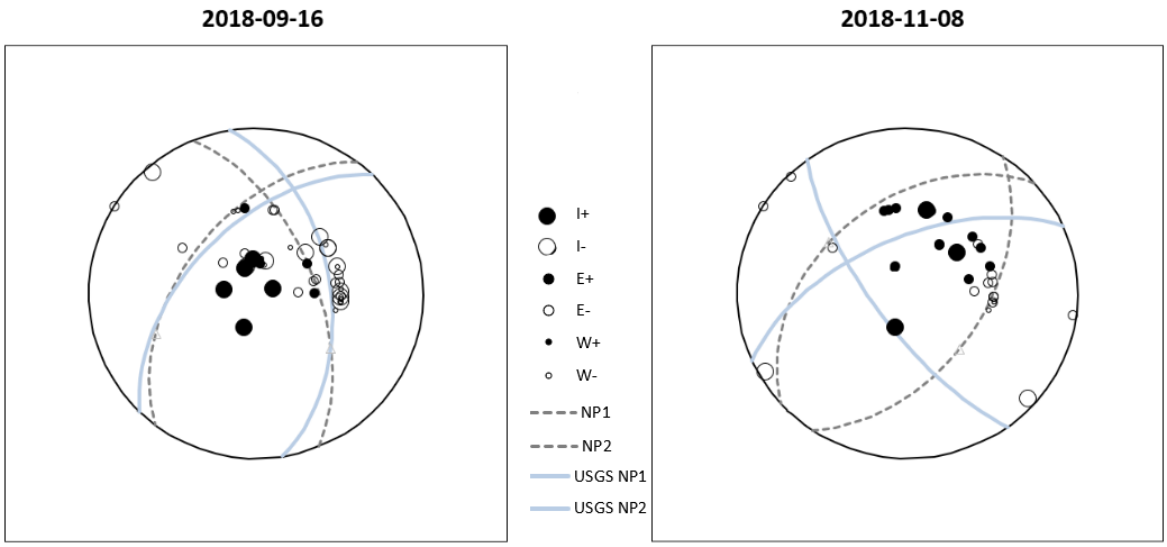

5 DISCUSSION

The aftershocks recorded by the LM network indicate a major cluster of aftershocks north of de Campos' farm about 3-4 Oct, and another concentration of activity about 7 km south associated with the ML 5.3 event on 8-9 Nov (near Johnson's farm). Lesser clustering in the vicinity of the "south farm" is suggested in late October 2018, and again in January 2019. The ML 5.3 event had several significant events in the hours preceding it (eg ML 3.8 at 1059 UTC, 10 hours earlier), and events on 4 and 6 November (both ML 2.4) may also be related. The few events surrounding the ML 5.7, 16 Sep 2018 event (to 19 Sep 2018) have not been analysed because, with no data from field stations, the locations are too poor. If considering only the October 2018 events, a nne trend could

be visualised on Figure 6, passing just to the east of de Campos' farm. This could be taken as support for the notion of a fault plane from the 16 Sep. event, dipping to the south-east but, overall, the distribution of epicentres does not seem to lend strong support for this interpretation.

The results indicate that epicentral trends can be masked by (sometimes significant) location errors. Relocations can be made using double difference techniques, as done by Clark et al. (2019), or by careful selection of the phase data used, as done in this report. Selecting the correct earth model is also an important factor, which has not been fully explored. The results of Clark et al. (2019), and this report, suggest that epicentral trends can be enhanced by relocations. Data presented in this report suggest a closer connection to the mapped (16 Sep.) rupture surface, but a trend related to the proposed northeast trending strike slip (8 November) fault could also be interpreted. The existing data set has not been fully utilised and there is scope for further analysis. In particular, the effect of using different earth models on the locations and focal depths should be investigated. Significant uncertainties remain in the focal depths presented, both by this study and that of Clark et al. (2019). All that can be confidently stated is that they are probably shallower than 5 km depth.

This is an example of moderately large earthquakes occurring in a region of low seismic hazard. It demonstrates the caution needed when using probabilistic earthquake risk maps to indicate the likely location of future large earthquakes.

5 Acknowledgements

Many thanks to Dan Clark and others at Geoscience Australia for assistance with this report. Thanks also to the assistance of Sean Standen and the staff of the Seismology Research Centre, Melbourne.

6 REFERENCES

Bowman, J. R. (1992). The 1988 Tennant Creek, Northern Territory, earthquakes: a synthesis, Australian Journal of Earth Sciences, 39, 651-669, 1992.

Burbidge, D. R., M. Leonard, D. Robinson, and D. Gray (2012). The 2012 Australian Earthquake Hazard Maps, in: The 2012 Australian Earthquake Hazard Map, D. R. Burbidge (Editor), 54-69.

Clark, D. J., S. Brennand, G. Brenn, T. I. Allen, M. C. Garthwaite, and S. Standen (2019). The 2018 Lake Muir earthquake sequence, southwest Western Australia: rethinking Australian stable continental region earthquakes, Solid Earth Discussion papers, *in review*. https://doi.org/10.5194/se-2019-125.

Dent, V.F. (1989). Computer generated crustal models for the southwest seismic zone, Western Australia. *Bur. Min. Res. Aust. Report* 1989/43.

Dent, V. F. (2016). A preliminary map of cluster locations in southwest Western Australia, 1990 - 2016 *Proceedings of the Australian Earthquake Engineering Society Conference, 2016, Melbourne.*

Dent, V. F. and Love, D.N., (2018). A review of seismicity in the Norseman region of Western Australia, 1970 – 2018. *Proceedings of the Australian Earthquake Engineering Society Conference, 2018, Perth.*

Dentith, M. C., Dent, V. F., and Drummond, B. J. (2000). Deep crustal structure in the southwestern Yilgarn Craton, Western Australia. Tectonophysics, 325, 227-255.

Doyle, H. A. (1971). Seismicity and structure in Australia, Bulletin of the Royal Society of New Zealand, 9, 149-152.

Gibson G., Wesson W., and Jones T. (1994). The Eugowra NSW Earthquake Swarm of 1994, *Australian Earthquake Engineering Society 1994 Conference Proceedings,* Canberra, pp. 71-80.

Leonard, M., (2003). Respite leave Burakin quaking in anticipation *AusGeo News* 70, June 2003.

Salmon, M., Kennett, B. L. N., and Saygin, E. (2013). Australian Seismological Reference Model (AuSREM): crustal component. Geophysical Journal International, 192, 1, 190-206. https://doi.org/10.1093/gji/ggs004

Somerville, P. & Ni, S. (2010). Contrast in Seismic Wave Propagation and Ground Motion Models between Cratonic and Other Regions of Australia. *Proceedings of the Australian Earthquake Engineering Society Conference, 2010, Perth.*

Waldhauser, F. & Ellsworth, W. L. (2000). A Double-Difference Earthquake Location Algorithm: Method and Application to the Northern Hayward Fault, California. Bulletin of the Seismological Society of America, vol. 90, no. 6, pp. 1353-1368.